Cross-Regional Marine Ecological Risk Assessment System Integrating Federated Learning

Xiao Lin[1], Qingyou Zhang[1], Shizheng Tian[2], Xinchang Guo[3]
[1]School of International Affairs and Public Administration, Ocean University of China, Qingdao, 266100, Shandong, China
[2]School of Marxism, Ocean University of China, Qingdao 266100, Shandong, China
[3]The Institution for Maritime Development Studies, Ocean University of China, The Humanities and Social Science Key Research Base of Ministry of Education, Qingdao 266071, Shandong, China

Corresponding author: Xinchang Guo (e-mail: gxc9205@ouc.edu.cn)

ABSTRACT Traditional centralized assessment methods often show bias in global modeling and struggle to balance knowledge sharing with local adaptation when cross-regional data are heterogeneous and non-independent and identically distributed. This problem is common in marine ecological monitoring and is also relevant to distributed electromagnetic sensing networks, where observation standards, sensor density, and local environments vary across regions. To improve the accuracy, consistency, and robustness of cross-regional marine ecological risk assessment, this paper proposes a system incorporating a hierarchical federated learning framework. Each client locally uses a hybrid model integrating physical mechanisms and data-driven capabilities, focusing on phytoplankton-nutrient-dissolved oxygen coupling dynamics. To maintain shared learning consistency, the system applies domain-adaptive regularized aggregation and aligns client hidden-layer distributions on the server, thereby mitigating feature drift. A lightweight personalized calibration layer compensates for regional heterogeneity. Characteristic variables are finally fused into a unified risk scale through uncertainty weighting to produce interpretable results. The method achieves an MSE of 0.483, an MMD of approximately 0.126, and a maximum regional variance of only 0.037, demonstrating stronger cross-regional stability and accuracy than baseline methods while preserving privacy. The system offers quantitative decision support for marine governance and provides a transferable framework for distributed sensor and electromagnetic monitoring applications.

INDEX TERMS marine ecological risk assessment, federated learning, domain adaptation, distributed sensing, electromagnetic monitoring networks

I. INTRODUCTION

MARINE ecosystems are facing increasing pressures from multiple sources, including climate change, landbased pollution, and human disturbance. Accurate assessment of their ecological risks is crucial for developing effective conservation policies and achieving sustainable management. However, current risk assessment practices face a fundamental obstacle: monitoring data is highly fragmented across different coastal areas, with significant differences in observation standards, sampling frequencies, and environmental contexts [1,2]. This "data silo" phenomenon not only hinders the identification of global risk trends but also makes it difficult to generalize experiences from a single region to others. More critically, due to privacy regulations and data sovereignty restrictions, raw environmental data is often not centrally shared, making traditional modeling methods relying on global data fusion difficult to apply.

Existing research on marine ecological risk assessment mainly focuses on data integration and model construction, forming a relatively rich theoretical and methodological system [3,4]. Fallati Luca used drones combined with multi-temporal and spatial-scale data of motion structures and object-based image analysis to conduct multi-temporal monitoring of shallow coral reef matrices in the Maldives, providing a feasible solution for assessing the impact of marine bleaching and ecosystem changes. At the model level, the application of machine learning and deep learning has promoted the intelligent development of risk prediction [5]. Adeoba Mariam I systematically sorted out the application of artificial intelligence (AI) in the field of marine waste management and ecological risk assessment through bibliometric analysis. The study found that AI algorithms and machine learning prediction models have great potential in pollution monitoring, hotspot prediction, and intelligent governance, and can become a key driving force for sustainable ocean management [6]. Goodwin Morten applied the application of supervised learning methods based on Deep Neural Network (DNN) in marine ecosystem management. Combining cases such as plankton, fish, marine mammals, and pollution, he demonstrated the mature and emerging applications of the model in species detection, classification, and tracking, and promoted the development of intelligent marine ecological monitoring and management [7]. These studies have improved prediction accuracy and risk identification capabilities to a certain extent, but they generally face problems of distribution offset, data privacy, and insufficient model generalization in crossregional applications. In this context, cross-regional marine ecological risk assessment integrated with FL has gradually become a new research direction. FL can achieve multi-regional collaborative modeling and knowledge sharing while ensuring local data storage and privacy security in each region, thus providing a new technical path for cross-regional ecological risk assessment [8-10]. These studies have demonstrated the potential of FL in crossregional modeling, but they are still mostly at the level of concept verification or local application, lacking systematic exploration for complex marine ecosystems. Especially in cross-regional marine risk scenarios, how to solve the distribution offset problem caused by inconsistent monitoring standards and non-stationarity of ecological processes, how to achieve dynamic domain alignment and personalized calibration in model aggregation, and how to combine uncertainty quantification to generate cross-regional unified risk indexes and spatial maps are still research gaps that need to be addressed.

To address these gaps, this paper constructs a domain-adaptive federated learning system for marine ecological risk assessment. Using FL as the overall framework, this system enables multi-region collaborative modeling while ensuring local storage and privacy security of regional data. The innovations of this paper lie in: addressing inconsistent standards and distribution shifts, a domain-adaptive regularization mechanism is introduced during the federated aggregation phase to enforce alignment of hidden layer feature distributions across regions, suppressing model bias due to differences in measurement systems; addressing the nonstationarity of ecological processes, a physically constrained hybrid model is constructed locally on the client, integrating the phytoplankton-nutrient-dissolved oxygen coupled kinetic equation with a DNN to capture regionally specific nonlinear responses while ensuring that the output conforms to ecological laws; addressing the needs of ecological risk assessment and uncertainty management, a lightweight, personalized calibration layer is designed, combining uncertainty estimation with a hierarchical aggregation strategy to generate an interpretable unified risk index. This paper not only fills the gaps in existing cross-regional ecological risk assessment methods in terms of distribution alignment and privacy protection, but the principles of its federated approach also provide new data-driven ideas and crucial technical support for complex, decentralized governance challenges. These challenges are found in many sectors, including the management of largescale supply chains like the industry, supporting effective cross-regional environmental governance and collaborative policy formulation across disparate operational sites.

II. CONSTRUCTION OF A CROSS-REGIONAL MARINE ECOLOGICAL RISK ASSESSMENT SYSTEM INTEGRATING FEDERATED LEARNING

The system uses a three-tiered federated architecture, as shown in Figure 1. On the left are multiple coastal regional clients; in the middle is the federated coordination server; on the right is the decision visualization. All raw observation data remains locally, with only encrypted gradients and aggregated statistics uploaded.

The proposed cross-regional marine ecological risk assessment system adopts a three-tier federated architecture, comprising edge clients, a federated coordination server, and a decision support interface. Bidirectional communication between the client and server is achieved via a TLS-encrypted gRPC interface. Model parameter updates, statistical moments, and calibration signals are transmitted in Protocol Buffers serialization format. Data adapters are deployed locally in each region to pull raw data from existing marine observation platforms in real time. After the raw data enters the local federated client, unit unification, outlier filtering, spatiotemporal interpolation, and quarterly resampling are performed sequentially. All preprocessing modules are encapsulated as Docker containers for easy deployment on edge devices or cloud nodes. This paper adopts a hierarchical federated learning architecture primarily due to the dual heterogeneity of cross-regional marine ecosystems: on the one hand, adjacent coastal areas share strong similarities in hydrological conditions, nutrient input, and plankton communities; on the other hand, distant regions exhibit significantly different ecological dynamics. If a single global aggregation is used, the model is easily dominated by areas with large data volumes or severe distributional shifts, leading to underfitting of small-scale or ecologically unique regions. Therefore, this paper designs a two-layer federated structure: the first layer is intra-regional aggregation, grouping geographically proximate monitoring stations with similar ecological characteristics into a subgroup for local model fusion; the second layer is cross-regional global aggregation, coordinating representative models from each subgroup to generate a unified risk assessment benchmark. Grouping is based on a comprehensive consideration of geographical proximity, correlation of ecological indicators, and consistency of monitoring standards.

A. DATA STANDARDIZATION AND SPATIOTEMPORAL ALIGNMENT

In a cross-regional marine ecological risk assessment system integrated with FL, due to the independent construction of regional marine environmental monitoring systems, significant differences in indicator definitions, and observation frequencies, this paper maps marine environmental moni-

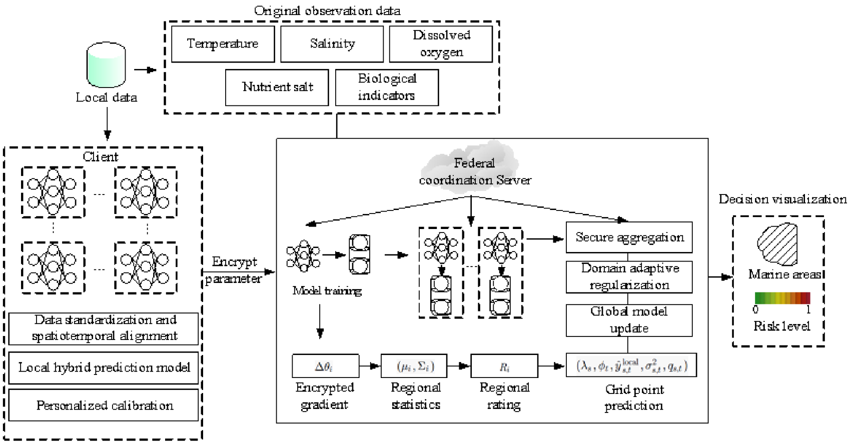

FIGURE 1. Trans-regional marine ecological risk assessment system framework

toring data collected from different regions into a unified feature space and spatiotemporal reference frame at the local end of the federated framework to avoid bias in global model parameter aggregation. This provides robust input for subsequent domain-adaptive regularization and personalized calibration layers.

First, unit conversion and baseline correction are performed on the five original variables of temperature, salinity, dissolved oxygen, nutrients, and biological indicators in each region to ensure that the values are in the same physical dimension. For observations of the same variable using different instrument systems, a linear calibration model is constructed using overlapping sample intervals:

$$x^{(j)} = ax^{(i)} + b + \epsilon \tag{1}$$

Least squares estimation is used to obtain a and b for cross-calibration; local weighted regression is used to map any nonlinear deviations. This calibration utilizes only local overlapping sample estimates; the server only receives model parameters or aggregated error statistics to protect privacy. In ocean monitoring, outliers arise from sensor drift, network packet loss, and extreme ecological events. This paper employs robust statistical metrics to label and remove anomalies. A Hampel filter is applied to single-point sequences:

$$\mathrm{MAD} = \mathrm{median}\left(|x_i - m|\right), \quad m = \mathrm{median}(x_i) \tag{2}$$

If $|x - m| > \mathrm{MAD}$, it is marked as abnormal. For time series mutations, the local median and local trend tests based on sliding windows are further used to retain ecologically significant extreme values and eliminate sensor noise. In view of the widespread problem of missing measurements in various regions, in the face of non-uniform sampling and intermittent observations, interpolation methods that retain space-time correlation are preferred. Locally, spatiotemporal interpolation based on Gaussian Process (GP) is preferentially performed [11]:

$$\hat{x}_* = k_*^T \left(K + \sigma_n^2 I\right)^{-1} y \tag{3}$$

σ_n^2 is the variance of the observation noise. GP includes a built-in uncertainty estimate, $\mathrm{Var}(\hat{x}_*)$, which serves as a confidence indicator for subsequent model inputs. For large-scale gridded fields, block kriging is preferred locally to balance efficiency and accuracy. The interpolation process is performed locally only, with the interpolated mean and variance reported to the server for cross-domain fusion.

Marine ecological processes are temporal [12-13]. This paper unifies the temporal reference and temporal resampling, defines a unified temporal resolution Δt as a quarterly scale and a reference starting point t_0, and maps each node observation to a unified time grid $t_j = t_0 + j\Delta t$ through resampling. If there is a frequency difference, linear interpolation is used:

$$\hat{x}(t_*) = \frac{t_2 - t_*}{t_2 - t_1} x(t_1) + \frac{t_* - t_1}{t_2 - t_1} x(t_2) \tag{4}$$

Seasonal-trend decomposition is performed on data with seasonal components:

$$S(t) = \sum_{m=1}^{M} \left(\alpha_m \cos \frac{2\pi mt}{T} + \beta_m \sin \frac{2\pi mt}{T}\right) \tag{5}$$

$$x'(t) = x(t) - S(t) \tag{6}$$

By removing significant seasonal cycles, temporal patterns across domains are made comparable, and distribution drift caused by periodicity is reduced. All observations are unified to the WGS84 (World Geodetic System 1984) reference coordinate system and mapped to a common spatial grid. Let the mapping function $g : (\mathrm{lat}, \mathrm{lon})$ project the coordinates into a grid index c. Observations within the grid are statistically summarized over the same time window:

$$\bar{x}_{c,t} = \frac{1}{|S_{c,t}|} \sum_{i \in S_{c,t}} x_{i,t} \tag{7}$$

$$\mathrm{Var}_{c,t} = \frac{1}{|S_{c,t}|-1}\sum_{i\in S_{c,t}}(x_{i,t}-\bar{x}_{c,t})^2 \tag{8}$$

For spatial interpolation requiring higher precision, Kriging weights are used:

$$\hat{x}(s_0) = \omega^T x \tag{9}$$

$$\omega = C^{-1}c \tag{10}$$

Under the premise of ensuring privacy protection, unified standardization is performed on each node based on global statistics. To balance comparability and privacy, secure aggregation is used to calculate the global mean and variance:

$$\mu_G = \frac{\sum_k n_k \mu_k}{\sum_k n_k} \tag{11}$$

$$\sigma_G^2 = \frac{\sum_k n_k\left(\sigma_k^2+\mu_k^2\right)}{N} - \mu_G^2 \tag{12}$$

Each site performs a global z-score normalization $x' = (x-\mu_G)/\sigma_G$ accordingly. When facing a strong-tailed distribution, robust normalization $x' = (x-\mathrm{median})/\mathrm{IQR}$ is used to reduce the impact of extreme values.

B. CONSTRUCTION OF LOCAL HYBRID PREDICTION MODEL

To achieve the dual goals of knowledge sharing and regional adaptation in cross-regional marine ecological risk assessment, this paper constructs a hybrid prediction model that integrates physical mechanism constraints and data-driven capabilities locally on each client of the FL framework. As shown in Figure 2, it consists of a physical constraint approximator and a DNN subnet. The former guides the learning direction of the neural network through physical priors to ensure that the model output conforms to the basic dynamic laws of the marine ecosystem; the latter is responsible for capturing complex nonlinear relationships and interactions with local characteristics, thereby generating risk prediction results that are both scientifically interpretable and highly generalized without relying on centralized data, and simultaneously outputting quantitative uncertainty estimates.

To clarify the integration method of physical mechanisms and data-driven models, a physical constraint approximator, as a fundamental component of the model, explicitly simulates the evolutionary trend of the marine ecosystem based on the phytoplankton-nutrient-dissolved oxygen coupling kinetic equation, outputting state predictions that conform to basic ecological laws. Phytoplankton biomass dynamics are analyzed using a modified Monod growth model, which considers the nonlinear effect of temperature on photosynthetic rate and introduces a natural mortality term. The nutrient consumption mechanism is assumed to be based on a proportional uptake relationship for phytoplankton, with the consumption rate being directly proportional to biomass and nutrient concentration. The dissolved oxygen balance process integrates two opposing processes: oxygen production from photosynthesis and oxygen consumption from respiration, resulting in net oxygen change. A deep neural network subnetwork serves as a compensation module, specifically learning the region-specific nonlinear biases and complex interaction effects that the physical model fails to fully characterize. The two are integrated additively. Physical constraints are introduced during training, and a loss function penalizes predictions that violate ecological laws. Through structural coupling and constraint-guided strategies, the organic synergy between the mechanistic model and the datadriven method is achieved.

This paper focuses on the dynamic coupling of phytoplankton, nutrients, and dissolved oxygen, as this is the core mechanism of nearshore eutrophication and hypoxia risk, and can effectively integrate the indirect effects of external pressures such as water temperature and pollutants. However, due to limitations in the availability and consistency of cross-regional data, including more variables exacerbate the problem of non-independent and identically distributed variables and reduce model robustness. The physical constraint approximator is constructed based on the classical dynamic equations of the marine ecosystem, using biomass P, nutrient concentration N, and dissolved oxygen concentration DO as state variables to construct a simplified phyto plankton growth-nutrient consumption-oxygen consumption metabolic coupling system. For phytoplankton growth and loss, there is:

$$\frac{dP}{dt} = \delta_{\max}\cdot f(T)\cdot\frac{N}{G_N+N}\cdot P - m\cdot P \tag{13}$$

$\delta_{\max}$ is the maximum specific growth rate; $f(T) = e^{\alpha(T-T_{\mathrm{ref}})}$ is the correction function of temperature on growth; G_N is the half-saturation constant; m is the natural loss rate of phytoplankton. For nutrient consump tion, there is:

$$\frac{dN}{dt} = -\frac{1}{Y}\cdot\delta_{\max}\cdot f(T)\cdot\frac{N}{G_N+N}\cdot P \tag{14}$$

Y is the phytoplankton's absorption coefficient of nutrients. For dissolved oxygen changes, there is:

$$\frac{dDO}{dt} = \gamma\cdot\delta_{\max}\cdot f(T)\cdot\frac{N}{G_N+N}\cdot P - R_0\cdot e^{\beta T}\cdot P \tag{15}$$

The first term represents the release of oxygen through photosynthesis, with the proportionality coefficient γ reflecting the amount of oxygen produced per unit of biomass. The second term represents the oxygen consumption due to respiration, which increases with temperature, with R_0 being the baseline respiration rate and β being the temperature sensitivity coefficient. On the discrete time grids s and t, this can be approximated as:

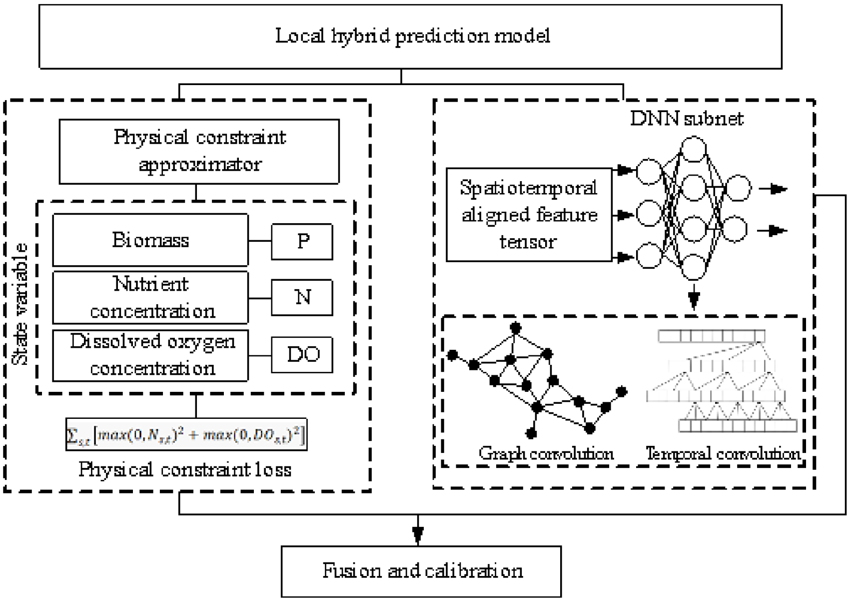

FIGURE 2. Local hybrid prediction model

$$DO^{\text{phys}}_{s,t+1} = DO_{s,t} + \Delta t \cdot [\gamma \cdot G(P_{s,t}, N_{s,t}, T_{s,t}) - R(P_{s,t}, T_{s,t})] \tag{16}$$

$G(\cdot)$ and $R(\cdot)$ are the growth and respiration terms, respectively. This simplified system characterizes the hypoxia mechanism caused by local nutrient overconsumption, providing physical and ecological rationality for risk assessment. To prevent model output from violating basic laws, a physical constraint loss is defined:

$$L_{\text{phys}} = \sum_{s,t} \left[\max(0, N_{s,t})^2 + \max(0, DO_{s,t})^2\right] \tag{17}$$

The nutrient and dissolved oxygen concentrations are constrained to be non-negative. To better simulate the nonlinear and multi-factor interactions existing in real ocean systems, a DNN subnetwork h_ϕ is introduced into the local model to compensate for the residual part that the physical approximator fails to cover [14-15]:

$$\tilde{y}^{\text{res}}_{s,t} = h_\phi(x'_{s,t}, N(s)) \tag{18}$$

The input is the normalized and spatiotemporally aligned feature $x'_{s,t}$, and $N(s)$ represents the neighborhood information of the grid s. This subnet uses a temporal convolutional structure to model temporal dependencies and captures spatial interactions through graph convolution. The local final prediction is formed by fusing the physical approximator with the neural subnet residual:

$$\hat{y}_{s,t} = g_\theta(x'_{s,t}) + \omega_{s,t} \cdot h_\phi(x'_{s,t}, N(s)) \tag{19}$$

$\omega_{s,t}$ is adaptively adjusted based on the uncertainty of the input data. When observations in a region are sparse or severely missing, the model relies more on the physical constraint approximator. When data quality is high, the weight of the deep subnet is increased to maintain robustness and reliability under different regional conditions.

To avoid point predictions masking the uncertainty of risks, a heterogeneous uncertainty modeling method is used to allow the network to directly output the predicted mean $\mu_{s,t}$ and variance $\sigma^2_{s,t}$, and optimize the negative log-likelihood:

$$L_{\text{nll}} = \frac{1}{2} \sum_{s,t} \left[\left(\frac{y_{s,t} - \mu_{s,t}}{\sigma_{s,t}} \right)^2 + \log \sigma^2_{s,t} \right] \tag{20}$$

C. SECURE AGGREGATION OF FEDERATED PARAMETERS

After the local hybrid prediction model completes training and outputs the risk prediction value and its uncertainty, this paper constructs a distributed parameter aggregation mechanism based on FL. By uploading only the gradient difference of model parameters, combining secure multi-party computing with domainadaptive regularization constraints, while protecting the data sovereignty of each region, it dynamically aligns the distribution of ecological characteristics of different sea areas, guiding the global model to gradually converge to a risk representation space with cross-regional consistency.

Each client locally computes the feature mean and covariance matrix of its model's intermediate layers and encrypts and uploads these high-order statistics to the server via a secure aggregation protocol. Without accessing the original data, the server synthesizes a global reference distribution using the statistics reported by all clients. This distribution represents the consensus representation of the cross-regional feature space in the current round. The server broadcasts this global reference matrix back to each client. Each client then locally computes the difference between its current hidden layer representation and the global reference distribution and constructs a regularized loss term. This loss term measures the distribution shift using the weighted sum of squared deviations of the feature mean and the Frobenius norm distance of the covariance matrix. This regularized term is incorporated into the local gradient update process, guiding the model to gradually converge towards a globally consistent feature space while preserving region-specificity. Finally, when aggregating model parameters, the server not only weights and averages the local model updates but also integrates the masked regularized gradients returned by each client, thereby optimizing the cross-domain distribution alignment objective at the parameter level. This process uses t as the index. Initially, the central server broadcasts the global basic model parameters θ_G^t to each grid s. Each grid area trains the local hybrid model with its processed input $x'_{s,t}$ to obtain the local parameters θ_s. The local parameter difference is defined as:

$$\Delta\theta_s = \theta_s - \theta_G^t \tag{21}$$

To suppress abnormal updates and ensure formal privacy guarantees, a Differential Privacy (DP) mechanism is integrated into the local update process. Specifically, after performing norm clipping on the parameter difference [16-17]:

$$\Delta\theta_s^{\text{clip}} = \frac{\Delta\theta_s}{\max\left(1, \|\Delta\theta_s\|/C\right)} \tag{22}$$

Gaussian noise $N(0, \sigma^2 C^2)$ is added to the clipped gradients, where the noise level σ^2 is adjusted according to the target privacy budget ϵ. This ensures that the aggregated global model does not leak sensitive information from any single regional dataset. During training, the noise scale σ varies within a predefined range (e.g., 0.1 to 5.0) to evaluate the system's sensitivity to privacy constraints.

C is the clipping threshold. Simultaneously, each region computes and (via a secure mechanism) prepares summary statistics for reporting: the local sample size n_s, the first-order feature moments μ_s and covariance Σ_s, and the local average prediction uncertainty $U_s = E_t[\sigma_{s,t}^2]$. These quantities are derived from local outputs and are used for subsequent domain alignment and weighting.

Each region masks its difference $\Delta\theta_s^{\text{clip}}$ and local statistics, so that the server can only get the sum after aggregation and cannot recover the value of a single client. The aggregated amount finally recovered by the server is the weighted difference [18-19]:

$$\overline{\Delta\theta} = \sum_s \alpha_s \Delta\theta_s^{\text{clip}} \tag{23}$$

$$\alpha_s \propto \frac{n_s}{N} \cdot \frac{1}{1 + kU_s} \tag{24}$$

It is normalized to make $\sum_s \alpha_s = 1$. The weighting strategy here combines the sample size n_s with the uncertainty U_s to reduce the undue influence of unreliable areas on the global model.

Simply averaging parameters may not eliminate systematic deviations in feature distribution across different regions. Therefore, a distribution alignment constraint based on feature moments is added during the aggregation phase. The server simultaneously obtains $\{\mu_s, \Sigma_s\}$ reported by each region through secure aggregation and constructs global reference moments $\mu_G = \sum_s \frac{n_s}{N}\mu_s$ and $\Sigma_G = \sum_s \frac{n_s}{N}\Sigma_s$. The distribution difference metric between each region and the global distribution is defined as:

$$D_s = \|\mu_s - \mu_G\|^2 + \|\Sigma_s - \Sigma_G\|_F^2 \tag{25}$$

The overall domain difference term is constructed [20-21]:

$$R_{\text{da}} = \sum_s \alpha_s D_s \tag{26}$$

Because the server cannot directly calculate the parameter gradients using raw samples, this paper implements domain-adaptive regularization using a collaborative two-step approach: the server first securely aggregates the global moment (μ_G, Σ_G) and broadcasts it to each region; each region locally evaluates the moment-sensitive gradient g_s of the local representation using the current global parameter θ_G^t; each region masks its gradient g_s and transmits it back; the server aggregates these local gradients to obtain the weighted regularized gradient $\bar{g}$. This approach ensures that the gradient calculation for domain alignment occurs locally, and the server only sees the aggregated gradient, thus balancing privacy and alignment. Based on the aggregated difference and domain-adaptive gradient, the server performs a one-step parameter update with regularization:

$$\theta_G^{t+1} = \theta_G^t + \eta\left(\overline{\Delta\theta} - \lambda g_{\text{da}}\right) \tag{27}$$

η is the learning rate, and λ_{da} is the domain adaptive regularization strength. This update is equivalent to applying a correction to the merged model in the parameter space to reduce the difference in feature distributions, thereby reducing the bias caused by cross-domain distribution drift in parameter aggregation. The client does not need to upload the original activation values or high-dimensional feature tensors; it only needs to calculate and encrypt the first and second-order statistical moments of its local hidden layer outputs after each training round. Furthermore, these can be transmitted in conjunction with the model gradient differencing, without introducing additional communication rounds. All high-dimensional alignment calculations are performed on the server side; the client only performs lightweight local moment calculations and regularized gradient backpropagation, enabling efficient execution on embedded monitoring devices or edge servers.

D. PERSONALIZED CALIBRATION AND LIGHTWEIGHT FINE-TUNING

After the federated parameters are securely aggregated to generate the global basic model θ_G^{t+1}, to address the contradiction between "global consistency" and "local adaptability" caused by the heterogeneity of ocean dynamics, differences in monitoring network density, and non-stationarity of ecological processes in various regions, this paper deploys a lightweight differentiable personalized calibration mechanism locally on the client.

When the global model θ_G^{t+1} is delivered to the i-th region, the system freezes all its core parameters—

including the dynamic parameters in the physical constraint approximator and the weights of the DNN subnet h_ϕ—and activates only a lightweight adaptation module attached before the output layer. This module consists of a single-layer fully connected network. Its input is the risk prediction value $\hat{y}_{s,t}^{\text{global}} = g_\theta(x'_{s,t})$ and its corresponding uncertainty output by the global model, and its output is the correction offset $\delta_i(x'_{s,t})$, which is in the form of:

$$\delta_i(x'_{s,t}) = W_i^{\text{cal}} \cdot \left[\hat{y}_{s,t}^{\text{global}}, \log\left(\sigma_{s,t}^2 + z\right)\right]^T + b_i^{\text{cal}} \tag{28}$$

$W_i^{\text{cal}} \in \mathbb{R}^{1\times 2}$, $b_i^{\text{cal}} \in \mathbb{R}$ are two trainable parameters learned only for this region, and z is a very small positive number used to ensure the stability of numerical calculations. It uses uncertainty as a regulatory signal. When historical observations in a region are sparse or the environment fluctuates violently, the model tends to rely on more conservative offset adjustments. Conversely, with the support of high-quality data, the calibration layer can significantly correct systematic biases [22-23]. The calibration layer is trained using local supervised fine-tuning, and the loss function is weighted mean squared error, combining the constructed quality indicator $q_{s,t}$ and the output uncertainty:

$$L_{\text{cal.}i} = \sum_{s,t} \frac{q_{s,t}}{\sigma_{s,t}^2 + \epsilon}\left(y_{s,t} - \left(\hat{y}_{s,t}^{\text{global}} + \delta_i(x'_{s,t})\right)\right)^2 \tag{29}$$

$y_{s,t}$ represents the continuous risk index (r), which is derived through the fuzzy fusion of predicted key state variables. The weighting strategy gives higher weights to high-quality, low-uncertainty samples to prevent noise from dominating the fine-tuning direction and ensure robust convergence of the calibration process, as shown in Figure 3.

Figure 3 illustrates the application of personalized calibration in federal marine risk assessment. The scatter plot in Figure 3A shows that when prediction uncertainty is high, the calibration weight decreases overall, indicating that the model adopts a more conservative correction strategy in scenarios with large environ mental fluctuations or sparse observations. Furthermore, higher-quality index samples correspond to larger calibration weights, indicating that the personalized calibration mechanism prioritizes using highly credible data for bias compensation. This mechanism effectively prevents low-quality data from dominating the calibration process, thereby improving the robustness and rationality of risk prediction. The results in Figure 3B show that the uncalibrated global model exhibits systematic overestimation or underestimation in multiple regions, with the mean bias significantly deviating from zero. However, after calibration, the bias distribution shrinks, correcting for regional-specific errors to a certain extent.

To prevent catastrophic forgetting, knowledge distillation constraints are introduced. During fine-tuning, the calibrated output $\hat{y}_{s,t}^{\text{cal}} = \hat{y}_{s,t}^{\text{global}} + \delta_i$ and the original global output $\hat{y}_{s,t}^{\text{global}}$ maintain a similar trend in the unlabeled area, that is, minimizing the KL (Kullback-Leibler) divergence [24-26]:

$$L_{\text{KD}} = \text{KL}\left(N\left(\hat{y}_{s,t}^{\text{global}}, \sigma_{s,t}^2\right) \| N\left(\hat{y}_{s,t}^{\text{cal}}, \sigma_{s,t}^2\right)\right) \tag{30}$$

This constraint forces the calibration layer to perform only local shifts rather than reconstructing the entire distribution, ensuring that the generalization ability of the global model is not compromised. Fine-tuning uses mini-batch gradient descent to reduce communication and computing costs.

E. RISK INDEX GENERATION

Taking regional individual predictions as primitives, it integrates regional prediction results and uncertainty information step by step to construct a unified cross-regional risk index, and generates a risk distribution map through spatial interpolation and mapping methods. In each region s, the calibrated localized prediction is:

$$\hat{y}_{s,t}^{\text{local}} = \hat{y}_{s,t}^{\text{global}} + \delta_i(x'_{s,t}) \tag{31}$$

To transform it into a unified risk scale, this paper defines the local risk index:

$$R_{s,t} = \frac{\hat{y}_{s,t}^{\text{local}} - \min\left(\hat{y}^{\text{local}}\right)}{\max\left(\hat{y}^{\text{local}}\right) - \min\left(\hat{y}^{\text{local}}\right)} \cdot \omega_{s,t} \tag{32}$$

The denominator is normalized across regions to ensure that variables of different characteristic scales are comparable within the unified risk interval $[0, 1]$. An ecological warning threshold is set for each key state variable: a potential risk event is considered when dissolved oxygen concentration is below 2 mg/L; nutrient salt concentration is consistently above 1.5 times the seasonal average; or phytoplankton biomass (characterized by chlorophyll-a) shows an abnormal surge (exceeding the historical 90th percentile). These predicted variables (DO, Nutrients, and Chl-a) are first normalized and then aggregated into a continuous Risk Index ($r \in [0, 1]$) using a weighted fuzzy membership function. This continuous index serves as the primary regression target for the FL model, while the individual prediction errors for each state variable are reported as secondary supporting metrics. $\omega_{s,t}$ is the uncertainty adjustment weight, defined as [27-28]:

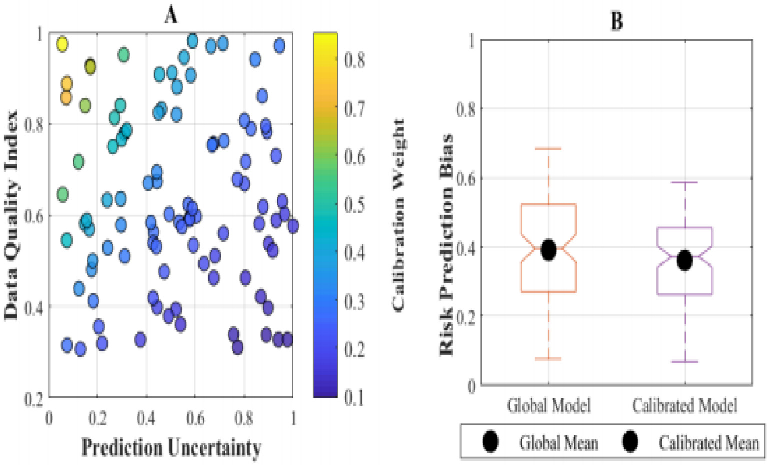

FIGURE 3. Weight Adaptation and Bias Reduction in the Federal Marine Risk Assessment: (A) shows the calibration weight distribution; (B) shows the bias comparison before and after calibration

$$\omega_{s,t} = \frac{q_{s,t}}{1 + k\sigma_{s,t}^2} \tag{33}$$

k is the adjustment coefficient. To form a unified cross-regional risk measurement, this paper adopts a two-level aggregation strategy: intra-regional time aggregation and cross-regional weighted aggregation.

Intra-regional time aggregation: the average risk level of a region in time period T is calculated:

$$\bar{R}_s = \frac{1}{|T|} \sum_{t \in T} R_{s,t} \tag{34}$$

The time average value ψ_s^2 of the uncertainty variance is combined as a robustness indicator to describe the long-term ecological risk exposure of the region. For cross-regional weighted aggregation, the $\bar{R}_s$ of multiple regions is integrated to generate a unified risk index $\bar{R}_{\text{UERI}}$:

$$R^{\text{UERI}} = \sum_{s=1}^{S} \alpha_s \bar{R}_s \tag{35}$$

After obtaining the risk index $\bar{R}_s$ of each region, a risk field based on geographic coordinates is constructed, and the uncertainty-weighted inverse distance weighted method is used to generate a continuous risk surface:

$$R(p) = \frac{\sum_s \frac{\bar{R}_s}{1+\psi_s^2} \cdot d(p, p_s)^{-\xi}}{\sum_s \frac{1}{1+\psi_s^2} \cdot d(p, p_s)^{-\xi}} \tag{36}$$

p is the location of the regional center p_s; $d(\cdot)$ is the geographical distance; ξ is the attenuation factor. By applying the uncertainty correction factor $(1+\psi_s^2)^{-1}$, the system weakens the impact of high uncertainty areas during spatial mapping and improves overall robustness.

III. VALIDATION OF CROSS-REGIONAL MARINE ECOLOGICAL RISK ASSESSMENT

A. EXPERIMENTAL SETUP

To ensure the objectivity of the experiment, this paper selects data from two databases, EMODnet (European Marine Observation and Data Network) Chemistry and Biology portals and NOAA (National Oceanic and Atmospheric Administration), as the experimental dataset. These two databases have long-term global and regional ocean observations and monitoring, providing long-term marine environmental and ecological obser vation data in different sea areas. During the data collation process, this paper standardizes the EMODnet and NOAA data at a unified quarterly temporal resolution, and divides them into eight subsets according to regional boundaries. The basic information of the data used is shown in Table 1:

TABLE 1. Experimental dataset

Classification	EMODnet Chemistry/Biology	NOAA
Coverage area	European coastal and adjacent waters	Globally
Main variable type	Nutrients, dissolved oxygen, chlorophyll-a, and plankton abundance integrated with Copernicus physical parameters (temperature and salinity)	Temperature, salinity, dissolved oxygen, plankton communities, and climate drivers
Sample size	14152 items	18366 items

To address the inconsistent spatiotemporal resolution of different data sources, a regional gridding method and bilinear interpolation are used to uniformly map the data to a 0.25° × 0.25° spatial grid and a seasonal time step. To systematically verify the effectiveness of the proposed cross-regional marine ecological risk assessment system integrating FL, a standardized federated training framework is constructed based on the dataset, with parameter settings shown in Table 2:

TABLE 2. Key parameter settings

Parameter	Specifications	Parameter	Specifications
Number of global communication rounds	50	Global learning rate	0.1
Client sampling rate per round	80%	Domain adaptive regularization	0.5
Local batch size	16	Privacy budget (ϵ)	0.1–5 ($\delta = 10^{-5}$)
Number of local training rounds	3	Gradient clipping threshold	1
Optimizer	Adam	Local model parameter count	≤1.2M

The comparative experimental design includes three types of baseline models, all of which are implemented within the same hierarchical (three-tier) structure—consisting of edge clients, regional aggregators, and a global server—to ensure a fair comparison: (1) Hierarchical-FedAvg, (2) Hierarchical-FedProx, and (3) Local Only. In these baselines, the intra-regional and cross-regional aggregation processes follow the same commu nication topology as the proposed system, with FedAvg and FedProx specifically applied as the local/global aggregation algorithms respectively.

(1) FedAvg: standard federated averaging without any distribution alignment or personalization mechanism;

(2) Local-Only: training a local model independently in each region without any parameter sharing, repre senting the “data island” benchmark;

(3) FedProx: a federated optimization method that introduces proximal terms to compare the superiority of domain adaptive regularization in this method.

Regarding evaluation dimensions, this paper develops from four dimensions: prediction accuracy, distribution alignment ability, model reliability (uncertainty calibration), and privacy protection effectiveness, and gener alization robustness.

Specific evaluation indicators include: prediction accuracy uses MSE and NMAE (Normalized Mean Absolute Error):

$$\mathrm{MSE} = \frac{1}{N}\sum_{i=1}^{N}(y_i - \hat{y}_i)^2 \tag{37}$$

$$\mathrm{NMAE} = \frac{1}{N}\sum_{i=1}^{N}\frac{|y_i - \hat{y}_i|}{\max(y) - \min(y)} \tag{38}$$

The distribution alignment ability is measured using MMD and KL divergence, where MMD is defined as:

$$\mathrm{MMD}^2 = \left\| \frac{1}{n_s}\sum_{i=1}^{n_s}\phi(h_i) - \frac{1}{n_t}\sum_{j=1}^{n_t}\phi(h_j) \right\|_H^2 \tag{39}$$

MMD is used to quantify the offset between the client and global latent space distributions; smaller values indicate better alignment.

Model Reliability: Expected Calibration Error (ECE):

$$\mathrm{ECE} = \sum_{b=1}^{B}|\mathrm{acc}_b - \mathrm{conf}_b| \cdot \frac{n_b}{N} \tag{40}$$

acc_b is the accuracy of the confidence interval, and conf_b is the corresponding average confidence level,

reflecting whether the predicted confidence intervals are well-calibrated and reliable.

Regional performance variance is defined as:

$$\mathrm{RPV} = \frac{1}{K}\sum_{k=1}^{K}\left(\mathrm{NMAE}_k - \overline{\mathrm{NMAE}}\right)^2 \tag{41}$$

This is used to assess cross-region performance consistency. Lower values indicate a more stable model for non-IID (Independent Identically Distribution) data. All metrics are calculated on a test set (20% of the total sample, divided independently by region) with five replicates, taking the mean and standard deviation to ensure robustness.

B. EXPERIMENTAL RESULTS

To protect data privacy, the Gaussian mechanism is employed for gradient perturbation. We implement Rényi Differential Privacy (RDP) as the accounting method to track the cumulative privacy loss across 50 communication rounds, ensuring the total budget remains within the specified ϵ range.

1) Prediction Accuracy

Regarding prediction accuracy, MSE and NMAE are employed to evaluate the regression performance of the continuous Risk Index (r). To provide a comprehensive assessment, we separately report the RMSE for the three underlying state variables (DO, Nutrients, and Chl-a). Furthermore, for the categorical risk levels derived from the index, ECE is utilized to assess the calibration of probability outputs, ensuring consistency between continuous regression and discrete classification evaluations. By comparing with the FedAvg, Local-Only, and FedProx baseline methods, whether the proposed method can significantly reduce risk assessment errors under the conditions of cross-regional data distribution differences is tested, and its advantages in unified modeling and regional adaptability are verified, as shown in Figure 4:

According to the convergence curve analysis results in Figure 4, the proposed method significantly outperforms the comparison methods in both prediction accuracy and convergence speed. In Figure 4A, the MSE index of the proposed method ultimately reaches 0.483, which is 25.0%, 31.5%, and 18.4% lower than FedAvg’s 0.644, Local-Only’s 0.705, and FedProx’s 0.592, respectively. In terms of the NMAE in Figure 4B, the proposed method exhibits lower error than other methods. This method introduces an improved federated optimization mechanism for cross-regional

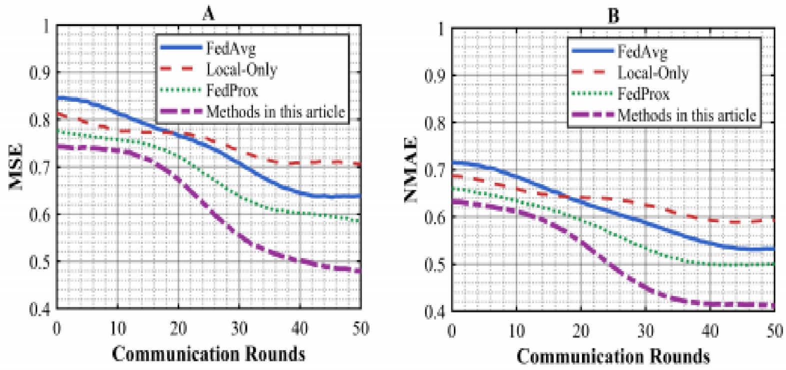

FIGURE 4. Comparison of MSE and NMAE: (A) shows the MSE results; (B) shows the NMAE results

marine ecological risk assessment, which can better coordinate heterogeneous data distribution across regions and reduce bias and oscillation during parameter aggregation. By combining regional feature weighting with multidimensional constraints, it effectively alleviates the performance degradation of traditional federated algorithms under data imbalance and complex environmental conditions, thereby achieving higher prediction accuracy.

2) Distribution Alignment Ability

In the distribution alignment evaluation, to quantify the consistency between the client model in each region and the global latent space distribution, this paper uses MMD and KL divergence as evaluation indicators. First, the MMD data of the eight subset regions is analyzed. The smaller the MMD value, the higher the degree of alignment between the client feature distribution and the global model. The comparison results are shown in Figure 5:

Figure 5 shows some differences in the MMD distributions of different methods across eight regions. As shown in Figures 5A, 5B, and 5C, the MMD values of the FedAvg, Local-Only, and FedProx methods exhibit significant fluctuations and a small number of outliers, reflecting the general alignment of client feature distributions with the global model across regions and limited cross-regional adaptability. In contrast, the proposed method (Figure 5D) achieves a significantly lower MMD, with a mean of approximately 0.126, minimal fluctuation, and few outliers, demonstrating its ability to efficiently align client latent space distributions with the global model and its cross-regional stability. The FL-integrated cross-regional marine ecological risk assessment system incorporates domain-adaptive regularization and personalized alignment strategies. While sharing global parameters, it fine-tunes local feature distributions, thereby reducing cross-regional distribution drift. KL divergence is further used to measure the difference between the distribution of marine ecological data in different regions and the global model distribution, and to evaluate the impact of cross-regional data heterogeneity on model training and risk assessment results, as shown in Figure 6:

In Figure 6, the proposed method achieves significantly lower KL values than other baseline methods across all regions, with an average KL divergence of 0.123, indicating more stable and consistent distribution alignment across clients. FedProx performs second best across all regions. While it introduces proximal constraints to mitigate the bias of local updates toward the global model, it fails to adequately account for cross-regional differences in the distribution of marine ecological risk characteristics, resulting in a higher KL divergence than the proposed method. Although FedAvg shares parameters through federated averaging, it does not account for inter-regional distribution heterogeneity and lacks adaptability to shifted distributions, resulting in a significant gap in KL performance. The Local-Only method trains each regional model independently without any global sharing or alignment mechanism, resulting in significant differences in the latent space between models across regions and high and unstable KL values. The proposed cross-regional marine ecological risk assessment system, integrated with FL, incorporates domain-adaptive regularization and a global-local collaborative optimization mechanism in its model design.

3) Privacy Protection Strength

In the model reliability assessment, the ECE metric is utilized to measure the deviation between the model risk assessment predicted probability distribution and the true distribution. To further analyze the trade-off between privacy and utility, we evaluate how the ECE (calibration performance) fluctuates as the privacy budget (ϵ) varies. Additionally, privacy protection strength is quantified by the Success Rate of Membership Inference Attacks (MIA) to ensure a rigorous evaluation of data confidentiality. With the privacy strength parameter as the horizontal axis and the different regions as the vertical axis, the method's ability to balance privacy protection and prediction credibility is verified, as shown in Figure 7:

Trade-off analysis: Impact of Privacy Budget on Model Calibration (ECE)

The results in Figure 7 show that the predicted probabil-

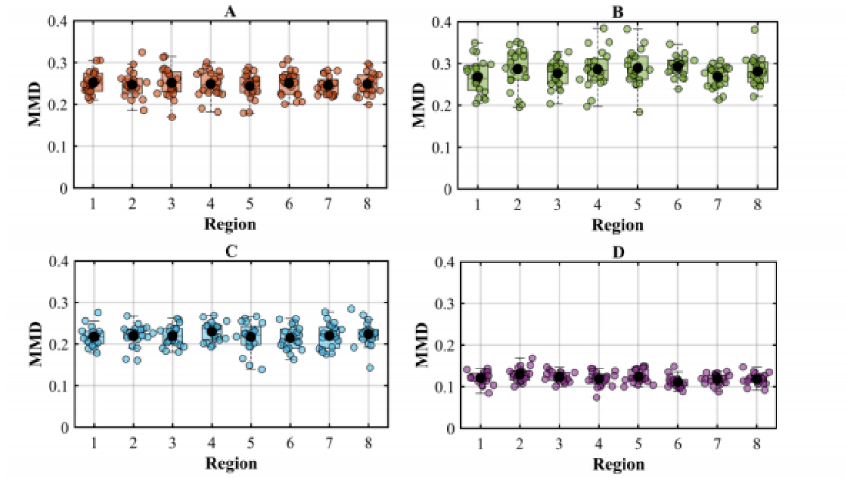

FIGURE 5. MMD Comparison: (A) FedAvg's MMD; (B) Local-Only's MMD; (C) FedProx's MMD; (D) The proposed MMD

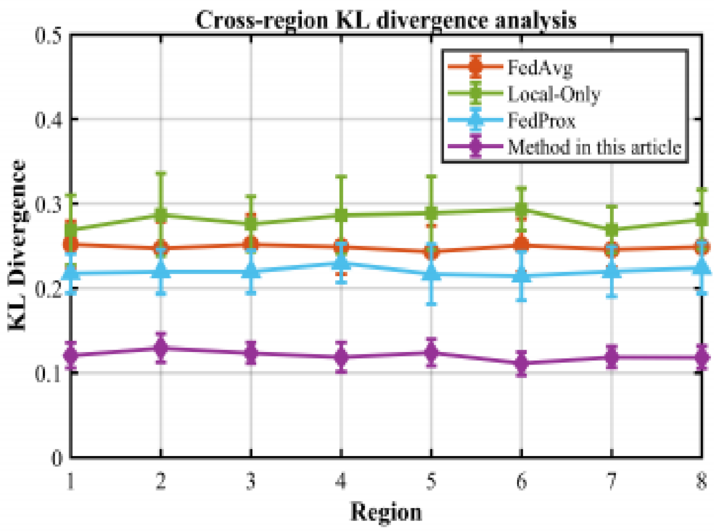

FIGURE 6. KL divergence comparison

ity distribution of the proposed model for ecological risk assessment is well aligned with the true distribution. The ECEs for FedAvg (Figure 7A) and Local-Only (Figure 7B) are generally high and fluctuate significantly across regions, demonstrating poor stability. FedProx (Figure 7C) mitigates the impact of inter-client variability on risk assessment to some extent, but still suffers from inaccuracies in some regions. In Figure 7D, the ECE of the proposed method is analyzed under varying privacy budgets ϵ. As shown in the performance-privacy trade-off curve, while the ECE remains relatively sta ble compared to baseline methods, a fundamental trade-off is observed: as the privacy protection strengthens (smaller ϵor higher noise σ), the ECE exhibits a slight upward trend and the prediction MSE increases. This is because the injected noise, while protecting privacy, inevitably interferes with the precision of local calibration signals. However, due to the introduction of the domain-adaptive regularization, our method maintains a lower ECE (under 0.05) even at high noise levels (σ= 2.0), demonstrating better robustness to privacyinduced perturbations than FedAvg.

4) Generalization Robustness

In marine ecological risk assessment, regional performance variance is used as an indicator to calculate the variance of each region's NMAE deviation from the overall mean. A low variance value means that the model can consistently and reliably assess the ecological risk of each region. The comparison results of various methods in a cross-regional scenario are shown in Figure 8:

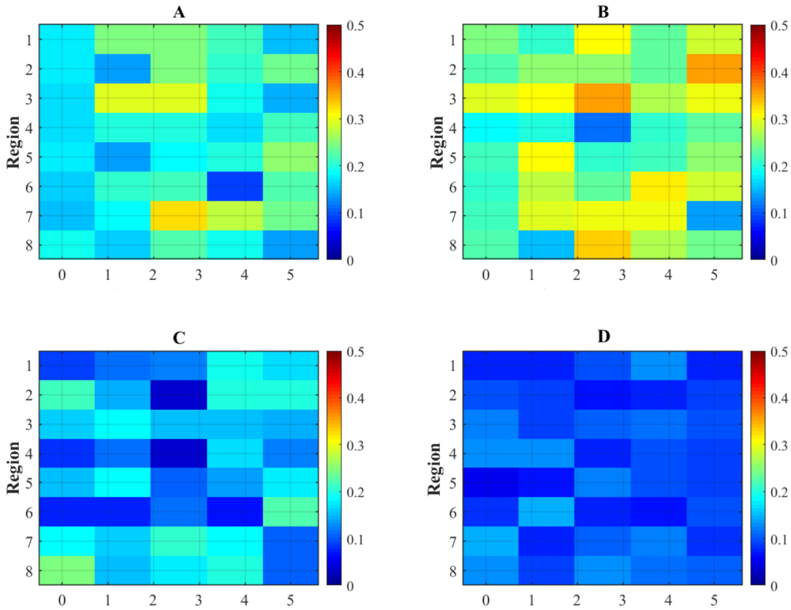

FIGURE 7. ECE Comparison: (A) shows the ECE of FedAvg; (B) shows the ECE of Local-Only; (C) shows the ECE of FedProx; (D) shows the ECE of the proposed method

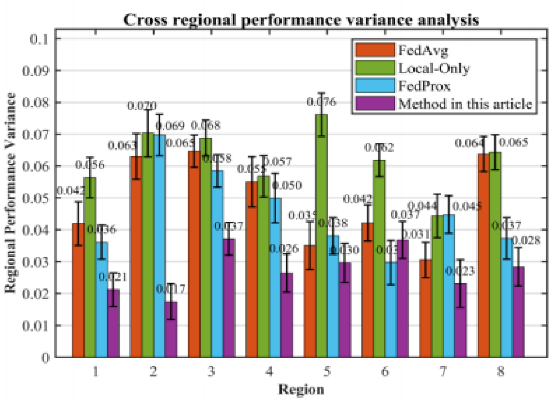

FIGURE 8. Regional performance variance comparison

Figure 8 shows the regional performance variance distribution of the proposed method, which clearly shows significantly lower variance across regions than the other compared methods, reaching a maximum of only 0.037. This indicates that the model's prediction performance fluctuates minimally across regions, demonstrating superior generalization robustness. In contrast, FedAvg and Local-Only exhibit higher variance in some regions, with Local-Only experiencing significantly increased variance fluctuations in a very small number of regions, reaching maximum variances of 0.065 and 0.076, respectively. This suggests that traditional methods are prone to localized performance degradation when dealing with non-IID data, leading to significant bias in marine ecological risk predictions in certain regions. FedProx improves regional performance consistency somewhat through constrained local updates, but still exhibits high variance in some regions, reaching a maximum of 0.069. The overall variance distribution remains higher than that of the proposed method.

IV. CONCLUSION

To address the challenges posed by cross-regional data heterogeneity, non-IID, and differential privacy constraints, especially considering the complex impacts of key industrial pollution sources such as the industry, and to improve the accuracy, stability, and privacy protection of cross-regional marine ecological risk assessment, this paper achieves cross-regional knowledge sharing through global local collaborative optimization based on the fusion FL framework. The production data (such as dye formula, water consumption) and pollution data of the industry have high sensitivity and commercial value. At the same time, the industry structure in different regions varies greatly, which greatly exacerbates the non- IID characteristics of data and the difficulty of privacy protection. Therefore, the framework proposed in this paper can collaboratively learn the deep correlation between production activities and marine ecological response in different regions without leaking the original data of various enterprises and environmental protection departments. Furthermore, person-alized calibration and domainadaptive regularization are introduced to construct a cross-regional assessment system that integrates FL. In comparative experiments, the proposed method demonstrates significant advantages in cross-regional marine ecological risk assessment: the final mean square error (MSE) value is 0.483, and the mean normalized mean error (NMAE) is significantly lower than that of the FedAvg, Local-Only, and FedProx baseline models. The distribution alignment metrics MMD and KL divergence perform well, indicating that the model's feature distributions are highly consistent across regions. In a regional performance variance comparison, the highest variance value is only 0.037, demonstrating strong generalization robustness. By leveraging personalized calibration, domain-adaptive regularization, and cross-regional distribution alignment strategies to effectively integrate heterogeneous data from diverse industrial clusters, this paper effectively improves the accuracy, stability, and privacy protection of marine ecological risk prediction, providing reliable technical support for regional collaborative management and scientific decision-making.

AUTHOR CONTRIBUTIONS

Conceptualization – Xinchang Guo; methodology – Xiao Lin, Qingyou Zhang, Shizheng Tian and Xinchang Guo; investigation – Xiao Lin, Qingyou Zhang, Shizheng Tian and Xinchang Guo; writing-original draft preparation – Xiao Lin, Qingyou Zhang, Shizheng Tian and Xinchang Guo. All authors have read and agreed to the published version of the manuscript.

CONFLICTS OF INTEREST

The authors declare no conflict of interest.

FUNDING

This research received no external funding.

ACKNOWLEDGEMENTS

Not applicable.

REFERENCES

[1] S. J. Painting, K. A. Collingridge, D. Durand, A. Gremare, V. Creach, C. Arvanitidis, et al., "Marine monitoring in Europe: is it adequate to address environmental threats and pressures? Ocean Science," 2020; 16(1): 235-252, doi: 10.5194/ os-16-235-2020.

[2] A. Melet, P. Teatini, G. Le Cozannet, C. Jamet, A. Conversi, J. Benveniste, et al., "Earth observations for monitoring marine coastal hazards and their drivers," Surveys in Geophysics, vol. 41, no. 6, pp. 1489-1534, 2020, doi: 10.1007/s10712-020-09594-5.

[3] F. Glaviano, R. Esposito, A. Di Cosmo, F. Esposito, L. Gerevini, A. Ria, et al., "Management and sustainable exploitation of marine environments through smart monitoring and automation," Journal of Marine Science and Engineering, vol. 10, no. 2, pp. 297-312, 2022, doi: 10.3390/jmse10020297.

[4] E. Buonocore, U. Grande, P. P. Franzese, and G. F. Russo, "Trends and evolution in the concept of marine ecosystem services: an overview," Water, vol. 13, no. 15, pp. 2060-2073, 2021, doi: 10.3390/w13152060.

[5] L. Fallati, L. Saponari, A. Savini, F. Marchese, C. Corselli, and P. Galli, "Multi-Temporal UAV Data and object-based image analysis (OBIA) for estimation of substrate changes in a post-bleaching scenario on a maldivian reef," Remote Sensing, vol. 12, no. 13, pp. 2093-2116, 2020, doi: 10.3390/rs12132093.

[6] M. I. Adeoba, T. Pandelani, H. Ngwangwa, and T. Masebe, "The Role of Artificial Intelligence in Sustainable Ocean Waste Tracking and Management: A Bibliometric Analysis," Sustainability, vol. 17, no. 9, pp. 3912-3942, 2025, doi: 10.3390/ su17093912.

[7] M. Goodwin, K. T. Halvorsen, L. Jiao, K. M. Knausgård, A. H. Martin, M. Moyano, et al., "Unlocking the potential of deep learning for marine ecology: overview, applications, and outlook," ICES Journal of Marine Science, vol. 79, no. 2, pp. 319-336, 2022, doi: 10.1093/icesjms/fsab255.

[8] J. Weber, M. Gurtner, A. Lobe, A. Trachte, and A. Kugi, "Combining federated learning and control: A survey," IET Control Theory & Applications, vol. 18, no. 18, pp. 2503-2523, 2024, doi: 10.1049/cth2.12761.

[9] H. Zhao, F. Ji, Y. Wang, K. Yao, and F. Chen, "Space-air-ground-sea integrated network with federated learning," Remote Sensing, vol. 16, no. 9, pp. 1640-1658, 2024, doi: 10.3390/rs16091640.

[10] A. Giannopoulos, P. Gkonis, P. Bithas, N. Nomikos, A. Kalafatelis, and P. Trakadas, "Federated learning for maritime environ ments: use cases, experimental results, and open issues," Journal of Marine Science and Engineering, vol. 12, no. 6, pp. 1034-1044, 2024, doi: 10.3390/jmse12061034.

[11] I. Achituve, A. Shamsian, A. Navon, G. Chechik, and E. Fetaya, "Personalized federated learning with gaussian processes," Advances in Neural Information Processing Systems, vol. 34, pp. 8392-8406, 2021.

[12] M. Daniels, S. van Vliet, and M. Ackermann, "Changes in interactions over ecological time scales influence single-cell growth dynamics in a metabolically coupled marine microbial community," The ISME Journal, vol. 17, no. 3, pp. 406-416, 2023, doi: 10.1038/s41396-022-01312-w.

[13] T. D. Eddy, J. R. Bernhardt, J. L. Blanchard, W. W. L. Cheung, M. Colleter, H. du Pontavice, et al., "Energy flow through marine ecosystems: confronting transfer efficiency," Trends in Ecology & Evolution, vol. 36, no. 1, pp. 76-86, 2021, doi: 10.1016/ j.tree.2020.09.006.

[14] S. Temitope Yekeen and A. L. Balogun, "Advances in remote sensing technology, machine learning and deep learning for marine oil spill detection, prediction and vulnerability assessment," Remote Sensing, vol. 12, no. 20, pp. 3416-3446, 2020, doi: 10.3390/rs12203416.

[15] Manso-Narvarte I , Solabarrieta L , Caballero A ,et al.Fishing vessels as met-ocean data collection platforms: data lifecycle from acquisition to sharing[J].Frontiers in Marine Science, 2025, doi: 10.3389/fmars.2024.1467439.

[16] Q. Chen, Z. Wang, J. Chen, H. Yan, and X. Lin, "Dap-FL: Federated learning flourishes by adaptive tuning and secure aggregation," IEEE Transactions on Parallel and Distributed Systems, vol. 34, no. 6, pp. 1923-1941, 2023, doi: 10.1109/ TPDS.2023.3267897.

[17] L. Zhao, J. Jiang, B. Feng, Q. Wang, C. Shen, and Q. Li, "Sear: Secure and efficient aggregation for byzantine-robust federated learning," IEEE Transactions on Dependable and Secure Computing, vol. 19, no. 5, pp. 3329-3342, 2021, doi: 10.1109/ TDSC.2021.3093711.

[18] X. Wang, Z. Liang, A. S. Voundi Koe, Q. Wu, X. Zhang, H. Li, et al., "Secure and efficient parameters aggregation protocol for federated incremental learning and its applications," International Journal of Intelligent Systems, vol. 37, no. 8, pp. -4487, 2022, doi: 10.1002/int.22727.

[19] Z. Yang, M. Zhou, H. Yu, R. O. Sinnott, and H. Liu, "Efficient and secure federated learning with verifiable weighted average aggregation," IEEE Transactions on Network Science and Engineering, vol. 10, no. 1, pp. 205-222, 2022, doi: 10.1109/ TNSE.2022.3206243.

[20] X. H. Ni, Z. L. Chen, H. Li, and X. J. Kong, "Anomaly identification and repair of hydrological telemetry data based on federated learning," Journal of Zhejiang University of Technology, vol. 51, no. 6, pp. 610-618, 2023.

[21] Z. Qin, J. Ye, J. Meng, B. Lu, and L. Wang, "Privacy-preserving blockchain-based federated learning for marine Internet of Things," IEEE Transactions on Computational Social Systems, vol. 9, no. 1, pp. 159-173, 2021, doi: 10.1109/TCSS.2021.3100258.

[22] A. T. Nguyen, P. Torr, and S. N. Lim, "Fedsr: A simple and effective domain generalization method for federated learning," Advances in Neural Information Processing Systems, vol. 35, pp. 38831-38843, 2022, doi: 10.52202/068431-2814.

[23] B. Sun, H. Huo, Y. Yang, and B. Bai, "Partialfed: Cross-domain personalized federated learning via partial initialization," Advances in Neural Information Processing Systems, vol. 34, pp. 23309-23320, 2021.

[24] X. Yu, D. Wang, M. J. McKeown, and Z. J. Wang, "Contrastive-enhanced domain generalization with federated learning," IEEE Transactions on Artificial Intelligence, vol. 5, no. 4, pp. 1525-1532, 2023, doi: 10.1109/TAI.2023.3298297.

[25] L. Yang, J. Huang, W. Lin, and J. Cao, "Personalized federated learning on non-IID data via group-based meta-learning," ACM Transactions on Knowledge Discovery from Data, vol. 17, no. 4, pp. 1-20, 2023, doi: 10.1145/3558005.

[26] W. K. Oestreich, M. F. Czapanskiy, K. Katija, et al., "Collective Science to Inform Global Ocean Protections," Ecology Letters, vol. 28, no. 8, Art. no. e70168, 2025, doi: 10.1111/ele.70168.

[27] L. Wu, S. Guo, Y. Ding, J. Wang, W. Xu, Y. Zhan, et al., "Re-thinking personalized client collaboration in federated learning," IEEE Transactions on Mobile Computing, vol. 23, no. 12, pp. 11227-11239, 2024, doi: 10.1109/TMC.2024.3396218.

[28] N. Purba, G. Faid, W. Zheng, et al., "Two centuries of oceanographic data in the Indonesian Seas and surroundings: historical patterns of data

availability, gaps, and future challenges," Earth System Science Data, vol. 17, no. 12, 2025, doi: 10.5194/essd-17-7203-2025.